Monitoring Field Lift Thickness Using Compaction Equipment Instrumented with Global Positioning System (GPS) Technology

Christopher L. Meehan[1]**; Mohammad Khosravi**[2]**; Daniel V. Cacciola**[3]

Abstract: When constructing earthen embankments, it is essential that the soil be placed and spread in uniform lifts prior to compaction. To ensure that the resulting soil lifts are evenly compacted, typical compaction specification approaches place restrictions on the thickness that is acceptable for each soil lift. In current practice, it can be extremely difficult for a field inspector to verify that lift thickness requirements are being met when soil is being placed and spread over a large area, without the use of frequent surveying (which adds both costs and delays to earthwork projects). Recent advances in compaction control include the development of continuous compaction control (CCC) and intelligent compaction (IC) systems, which provide real-time monitoring and feedback about the operation and performance of soil compaction. Typically, CCC and IC compaction equipment is outfitted with a real-time kinematic global positioning system (RTK-GPS) that monitors and records the position of the compacter as the soil lift is being compacted. This paper suggests that geotechnical engineers use field RTK-GPS measurements that are made by CCC or IC equipment to monitor and control the thickness of compacted soil lifts. Data collected from a full-scale field study is used to illustrate the practical issues with using GPS measurements for field monitoring of lift thickness during construction of a roadway embankment, such as varying roller position from lift-to-lift and the measurement uncertainty associated with RTK-GPS measurement data. The use of both simple and sophisticated spatial analysis techniques are explored for interpolating measured field elevation data onto a uniform grid for lift thickness assessment. The resulting methodology that is presented can be utilized to build spatial maps of compacted soil lift thickness, a process that can be used to great benefit by field engineers who are trying to ensure the quality of compacted soil lifts.

DOI: 10.1520/GTJ20120124

Keywords: Continuous compaction control; Earthwork; Compaction; Geostatistics; Lift thickness; Quality control; Quality assurance.

Reference: Meehan, C. L., Khosravi, M., and Cacciola, D. V. (2013). "Monitoring Field Lift Thickness Using Compaction Equipment Instrumented with Global Positioning System (GPS) Technology." *Geotechnical Testing Journal*, ASTM, 36(5), 755-767. (doi:10.1520/GTJ20120124)

Note: The manuscript for this paper was submitted for review and possible publication on June 25, 2012; approved for publication on June 21, 2013; and published online in July of 2013.

1 Introduction

Proper compaction of soil is necessary to ensure optimal strength and compressibility behavior. In current geotechnical engineering practice, the process of soil compaction in the field is typically monitored and controlled using quality-assurance and/or quality-control (QA/QC) procedures that control either the method of soil compaction, or the end-product that results after compaction has been performed. Both "method-based" and "end-product-based" specification approaches typically employ some control over the way in which soil is placed, spread, and compacted. Of particular importance for both of these specification approaches is a restriction on the thickness of each compacted lift. Typically, maximum allowable "loose-lift" or "compacted-lift" thicknesses are specified,

[1]Bentley Systems Incorporated Chair of Civil Engineering & Associate Professor, University of Delaware, Dept. of Civil and Environmental Engineering, 301 DuPont Hall, Newark, DE 19716, U.S.A. E-mail: cmeehan@udel.edu (corresponding author)

[2]Graduate Student, University of Delaware, Dept. of Civil and Environmental Engineering, 301 DuPont Hall, Newark, DE 19716, U.S.A. E-mail: khosravi@udel.edu

[3]Graduate Student, University of Delaware, Dept. of Civil and Environmental Engineering, 301 DuPont Hall, Newark, DE 19716, U.S.A. E-mail: dcacc@udel.edu

as keeping lifts from getting too thick helps to ensure optimum compactor energy penetration and a relatively uniform density of the final compacted soil lift.

Unfortunately, one of the easiest ways for a contractor to place fill more quickly is to push the boundaries on lift thickness requirements (another option is to finish compacting each lift with fewer overall compactor passes). For 15-cm to 30-cm compacted lifts, even pushing the lift thickness up by 2 to 4 cm can yield extremely significant cost savings over the course of a project (on the order of 10% or greater), especially for larger embankments or deeper fill areas. Further, in the field, it can be extremely difficult for an inspector to verify that lift thickness requirements are being met over a large area without regular surveying, which adds additional costs and delays to earthwork projects. The resulting situation is one that has significant potential for conflicts and ensuing litigation, in that contractors are financially incentivized to push the boundaries on lift thickness, whereas existing QA/QC procedures are generally ineffective for large-area field control.

Recent advances in compaction control include the development of continuous compaction control (CCC) and intelligent compaction (IC) systems, which provide real-time monitoring and feedback about the operation and performance of soil compaction (e.g., Thurner and Sandström 1980; Adam 1997; Adam and Brandl 2003). For vibratory compactors, the data that is often collected includes the vibratory frequency, the amplitude of the roller drum, and the speed of the roller (Adam 1997). For machine drive power-based systems, the gross power that is applied by the compactor is typically recorded, in addition to other properties such as roller speed, roller acceleration, and the slope angle (White et al. 2005). The data recorded by sensors on CCC and IC compaction equipment can be used to perform QA/QC of compacted soil, and current guidance exists for incorporating these measurements into an end-product-based specification framework (e.g., Mooney et al. 2010). A major advantage of the data that is recorded by CCC and IC systems is that measurements can be made much more continuously than with traditional spot-measurement tests such as the nuclear density gauge test or sand cone test. Consequently, CCC or IC measurements are sometimes considered to represent 100% coverage of the compacted area (e.g., Vennapusa et al. 2010).

Most CCC and IC compaction equipment is outfitted with real-time kinematic global positioning system (RTK-GPS) equipment (Vennapusa et al. 2010; White et al. 2011). The purpose of this on-board instrumentation is to record the location of each in situ indicator measurement that is made by the compacter in real time, such as the "compactometer value" (CMV) or "machine drive power" (MDP) value (e.g., Meehan and Tehrani 2011). Taken together, the compaction indicator measurements and their corresponding locations can be used to build spatial maps that identify areas where additional compaction effort is needed to ensure optimal end-product results.

Significant research has been performed to date to correlate the results from in situ spot testing to the different types of measurements that are made by CCC and IC equipment (e.g., Floss et al. 1983; Samaras et al. 1991; Brandl and Adam 1997; Thompson and White 2008; Tehrani 2009). Primarily, these studies have been focused on the effective use of CCC/IC equipment for verifying the end-product of the soil-compaction process. However, researchers have largely overlooked one of the most significant measurements that is being made by the instrumented compaction equipment, its three-dimensional position. More specifically, the position measurements that are made by the RTK-GPS instrumentation provide a mechanism for field engineers to monitor the process of soil compaction and the resulting thickness of compacted soil lifts across an entire compacted area. As the thickness of compacted soil lifts plays a critical role in both method-based and end-product-based compaction specifications, this new RTK-GPS "observation approach" adds a significant tool to the field engineer's toolbox. Most importantly, this tool allows for enhanced off-site monitoring, and has none of the prohibitive costs and schedule delays that are associated with field surveys.

This paper provides a framework for using field RTK-GPS measurements made by CCC or IC equipment to monitor and control the thickness of compacted soil lifts during construction of a roadway embankment. Data collected from a full-scale field study is used to illustrate the practical issues with using GPS measurements for field monitoring of lift thickness, such as varying roller position from lift-to-lift and the measurement uncertainty associated with RTK-GPS measurement data. The use of both simple and sophisticated spatial analysis techniques are explored for interpolating measured field elevation data onto a uniform grid for lift thickness assessment. The resulting methodology that is presented can be used to build spatial maps of compacted soil lift thickness in real time, a process that can be used to great benefit by field engineers who are trying to ensure the quality of compacted soil lifts. The proposed process is advantageous in that it can be conducted from remote locations, without the added costs and delays that would be associated with a formal field elevation survey.

2 Project Description

The field study described in this paper was performed at Burrice Borrow Pit in Odessa, DE in the United States. For purposes of this study, a 61-m-long by 6-m-wide (200 ft by 20 ft) embankment was constructed using conventional earth-moving equipment, following Delaware general specifications for road sub-base construction (DelDOT 2001). The soil that was used to construct the embankment was generally uniform (Meehan and Tehrani 2011), falling at the classification boundary between two soil types: a poorly graded sand with silt (SP-SM) and a silty sand (SM). This soil is a commonly used borrow material for the Delaware Department of Transportation (DelDOT), and it generally conforms to state "select fill" borrow specifications (DelDOT 2001).

The goal of the construction process for this study was to build the embankment to an approximate total final height of 0.9 m (3.0 ft), by compacting five 20.3 cm (8 in.) loose-lift layers. To construct each lift, a Caterpillar 980H bucket loader was used to place fill for spreading by an on-site bulldozer. A Caterpillar D6K dozer was then utilized for spreading the material to an approximate loose-lift thickness of 20.3 cm (8 in). The D6K dozer was equipped with a global positioning system (GPS), which proved beneficial for establishing a relatively uniform and consistent loose-lift thickness. After spreading each lift, a water truck was driven through the test area as needed to adjust the moisture content of the fill material to achieve optimum compaction.

Upon completion of loose-lift soil placement and moisture conditioning, each soil lift was compacted using a Caterpillar CS56 vibratory smooth drum roller. This prototype machine had been specially modified by Caterpillar research engineers to measure CCC values. It also utilized an onboard RTK-GPS to accurately establish the location of the compactor in real-time, as it made in situ measurements. In the current study, the receiver for the GPS unit was located above the center of the roller drum. The roller drum was 2.1 m (7 ft) wide, and had an operating weight of 11,414 kg (25,164 lb). During compaction, the roller speed was kept relatively constant, at around 3.25 km/h. In situ CCC measurements and X, Y, and Z position readings were made simultaneously approximately every 20 cm (8 in.) along the length of the test section (although in reality this measurement-interval distance was much more variable, as will be discussed in more detail in a subsequent section).

Using the modified Caterpillar CS56 compactor, each lift was compacted in a series of passes using three side-by-side lanes [the roller width was 2.1 m (7 ft), the test pad width was 6 m (20 ft), which left approximately 15 cm (6 in.) of overlap at the edges of each compacted soil "lane"]. For each lift, between six and nine compactor passes were performed to achieve the desired level of compaction. Measured CCC results from this study are discussed in more detail in a separate publication (Meehan and Tehrani 2011), and information from other in situ tests that were conducted is also discussed elsewhere (Meehan et al. 2012). The following sections describe an analytical framework for processing the measured GPS data to determine post-compaction lift thicknesses for field QA/QC.

3 An Approach for Monitoring Field Lift Thickness

The concept that is proposed in this paper is simple in nature: take the elevations (Z values) measured using the RTK-GPS from one lift, and compare those values to the measured RTK-GPS elevations from the previous lift. The difference between two elevation measurements at the same location is the lift thickness at that location. In practice, however, this comparison process is more complicated than it seems, as the CCC compactor is never at the same two locations in space (the same X and Y coordinates) from lift to lift. A mathematical way around this problem is to define a fixed-position (X, Y) coordinate grid, and to use interpolation from the RTK-GPS measured elevation values to determine the corresponding elevations at each of the grid points. Because the resulting elevation measurements for each lift are all interpolated onto the same fixed-coordinate X-Y grid system, the lift thickness at each grid point location can then be calculated by taking the difference in elevation from layer to layer from the overlying grids. This process is then repeated for each grid point over the entire area of compaction, to build a spatial map of lift thickness. This process is illustrated in more detail in the following sections, which demonstrate how commonly used interpolation approaches can be implemented within this framework to infer the spatial distribution of lift thickness for various compacted soil lifts.

For the process described previously to work properly, it is necessary to use geospatial statistical analysis tools for interpolating onto a fixed-coordinate grid. In geospatial statistical analysis, sample points taken at discrete locations in an area are used to predict values at desired locations in that area and create (interpolate) a continuous surface. The sample points can be measurements of any phenomenon, such as soil properties or elevation measurements.

Inverse distance weighting (IDW) and/or kriging techniques are commonly used to predict an unknown measurement value at a specific location from a known surrounding data set (e.g., Isaaks and Srivastava 1989). IDW is a deterministic interpolation technique that weights the contribution of neighboring measurement values depending upon their distance from each point of interest. Kriging techniques, in contrast, use much more sophisticated geostatistical characterization techniques to create interpolation surfaces that incorporate the statistical properties of the measured data. Although kriging is generally accepted as the "best linear unbiased predictor" (BLUP) from a mean-squared-error standpoint (e.g., Isaaks and Srivastava 1989, Cressie 1993), the IDW interpolation approach does offer some advantages in its simplicity, especially for rapid implementation by field engineers. Consequently, this paper will explore the use of both approaches for interpolation of gridded elevation values, and compare the results. For the research described here, the statistics program R was used to perform kriging and IDW interpolation (R Development Core Team 2011); a wide variety of other computer programs are also readily available to perform these computations.

4 Using RTK-GPS Measurements to Monitor Compactor Location

As noted in the previous section, this paper describes the results from a field study where five lifts of soil were compacted, with each lift needing multiple compactor passes. Figure 1 shows the measured RTK-GPS position data from the final compactor passes for each lift. Figure 1(a) shows the position of the compactor on each lift in plan view (following an X and Y coordinate system); the three lines that are shown on each plot correspond to the centerline of the three lanes of compaction that were performed over the area of construction for each lift. Figure 1(b) shows a profile view with the corresponding elevation (Z) values that were recorded along the line of compaction for each lift, for each of the three lanes of compaction. Note that data from lift 1 was not available because of a malfunction in the data-acquisition system. Consequently, the relatively large elevation gap between lift 0 and lift 2 in Fig. 1(b) corresponds to the thickness of two compacted lifts.

The data shown in Fig. 1 supports the authors' previous observation that the compactor can generally be in different locations from lift to lift. Also, it illustrates that there can sometimes be gaps or jumps in the data that is recorded, an undesirable phenomenon that may sometimes be observed for a variety of reasons on a real project site.

For many project sites, compactor position data will be recorded in Northings and Eastings via the GPS measurement system. For convenient gridding, it can be advantageous to convert this global X'-Y' coordinate system to a local X-Y coordinate system that generally corresponds to the longitudinal and transverse directions of the roadway section that is being analyzed. In this paper, we utilized a local roller coordinate system that is based on the general orientation of roller travel, i.e., with X in the direction of roller travel and Y along the axis of the drum (perpendicular to the roller travel direction). In the current project, X (the primary direction of roller travel) is aligned with the longitudinal dimension of the roadway earthwork section and Y is aligned with the transverse direction. The elevation values used throughout this study (Z) correspond to an arbitrary local datum. The data shown in Fig. 1 was converted to the local coordinate system that is shown using the following transformation matrix:

$$\begin{bmatrix} X \\ Y \end{bmatrix} = \begin{bmatrix} \cos\,\alpha & -\sin\,\alpha \\ \sin\,\alpha & \cos\,\alpha \end{bmatrix} \begin{bmatrix} X' \\ Y' \end{bmatrix} \tag{1}$$

where α is the rotation angle between the local coordinate system and the northing-easting coordinate system.

5 Establishing a Uniform Grid for Thickness Map Creation

To build an ideal map of lift thickness for each lift, it would be useful to have known elevation values measured at a regularly spaced grid interval. Because elevation data cannot be easily obtained in this format with conventional CCC/IC compaction equipment, it is instead much easier to project from the high-density map of recorded elevation values onto an artificially created grid. The effect of grid point spacing in this projection grid on the analysis results was one of the factors that was explored in this study.

The (X, Y) point density of the recorded RTK-GPS points is governed by the speed and direction of the compactor, as well as its data-acquisition frequency. The resulting spacing between neighboring points in the X and Y directions is somewhat variable. Figure 2 shows the cumulative distribution functions of the point spacings in the X and Y directions for each of the five lifts. The overall mean spacing of all of the measured values in the X direction is 0.18 m, and in the Y direction is 1.95 m. These recorded data spacings are typical for CCC projects of this type (e.g., Facas et al. 2010).

A thorough sensitivity analysis was performed to determine the most appropriate geospatial grid point spacing for elevation interpolation. A number of isotropic grid spacings were assessed, with equal point spacings in the X and Y directions of 0.01 m, 0.05 m, 0.1 m, 0.5 m, and 1.0 m. For isotropic projection grids with a spacing greater than 0.1 m, the grid point spacing that was selected was found to have a noticeable effect on the predicted elevation results. At grid point spacings less than or equal to 0.1 m, the predicted elevation results converged, with no additional change in results being observed at smaller grid point spacings. Consequently, an isotropic grid spacing of 0.1 m was selected for use in this study, as it is the most computationally efficient. This spacing is also a logical choice as it is near the lower bound of the measured point-spacing distances in the roller measured direction (the X direction, Fig. 2).

As the spacing of the measured data was relatively anisotropic in nature (Figs. 1 and 2), the use of an anisotropic grid-spacing pattern was also explored. An anisotropic grid with X and Y point spacings of 0.1 m and 1 m, respectively, generally yielded the same results as an isotropic grid with a 0.1 m point spacing. This observation supports the conclusion that the most important factor when selecting a projection grid is to use grid spacings in the X and Y directions that are smaller than the corresponding closest point spacings in the measured data. Although coarser grid point spacings can be used without an extremely large difference in results, there is no real reason to use a coarser grid, as the computational power of a conventional desktop computer can handle more refined grid spacings with ease. As the run times for a 0.1 m isotropic grid and an (0.1 m, 1 m) anisotropic grid were both fairly quick, an isotropic grid spacing of 0.1 m was arbitrarily selected for presentation of results in the current manuscript. (For the sake of brevity, results from many of the grid point "sensitivity studies" that were performed are not included here.)

6 Interpolation Using the Kriging Method

Kriging is a geostatistical interpolation method that predicts values at unmeasured locations (e.g., Isaaks and Srivastava 1989). Predicted values consider both the distance and the degree of variation by using a weighted linear combination of the sample measured values. Unlike other geostatistical tools, kriging does not apply the same weighting functions to all sample measured values. Instead, weighting functions are applied based on the distance and orientation of the sample measured values with respect to the location of the estimated value and the way in which the sample measured values are grouped. The assignment of these functions attempts to minimize the variance error and to obtain a value of zero for the mean of the prediction errors, to prevent over- or underestimation. There

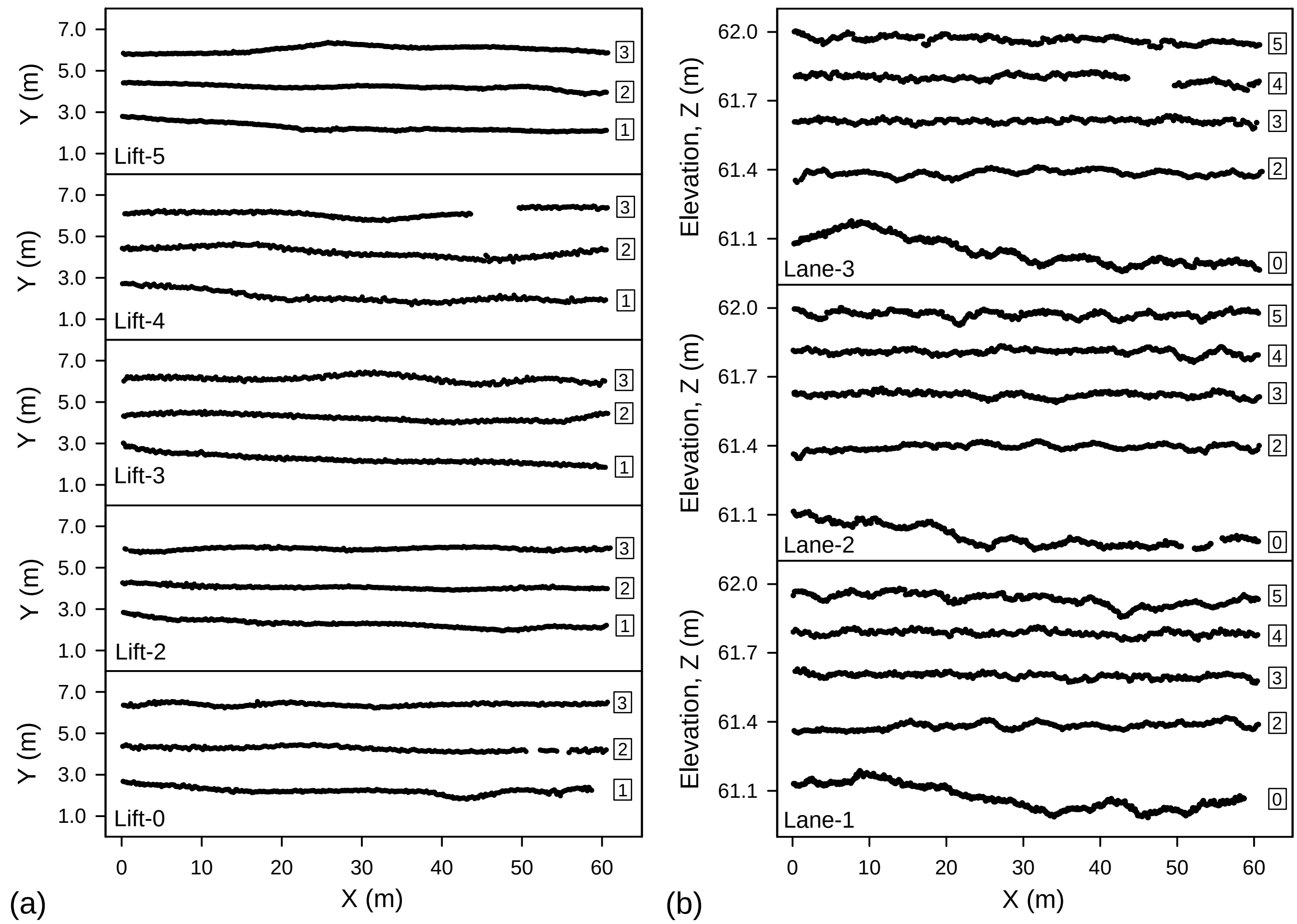

Fig. 1: RTK-GPS data measured by CCC equipment for five overlying lifts of compacted soil, with three lanes of compaction for each lift: (a) plan view, and (b) profile view.

are several different kriging techniques that are commonly used; for this study, ordinary kriging was selected. Ordinary kriging assumes that a data set has a stationary variance and also a non-stationary mean value within the sample measured values (e.g., Isaaks and Srivastava 1989).

6.1 *The Role of Semivariograms in Kriging*

A quantitative measure of the degree of spatial dependence between sample measured values can be made using the concept of empirical semivariance (e.g., Isaaks and Srivastava 1989; Cressie 1993; Clark and Harper 2002). The semivariance is computed by taking half the variance of the differences between measured values for all possible points in a data set that are spaced at a constant distance apart (Eq. 2). The empirical semivariogram $\gamma(h)$ is a plot of the semivariances as a function of different point spacing distances (Olea 2006).

$$\gamma(h) = \frac{1}{2N_h} \sum_{i=1}^{N_h} \left[z(x_i + h) - z(x_i)\right]^2 \tag{2}$$

where $z(x_i)$ is a measurement taken at location x_i, and N_h is the number of pairs h units apart in the direction of the vector (Olea 2006).

Empirical semivariogram plots are typically used to develop the weighting functions for kriging. Following conventional practice, a theoretical model $\gamma'(h, \theta)$ is fit to the empirical semivariogram $\gamma(h)$ data; this theoretical model is then used to determine the appropriate kriging weighting functions. A variety of theoretical semivariogram models are commonly used with ordinary kriging. For geospatial predictions, the four most common models are probably the linear, spherical, exponential, and Gaussian models (e.g., Isaaks and Srivastava 1989, Cressie 1993, Clark and Harper 2002). The "best" model for use with a given data set may be chosen by visual examination of the empirical semivariogram $\gamma(h)$ or using other statistical data-fitting techniques. For the current study, the model that was selected as the "best fit" from the empirical semivariograms was the Gaussian model, which is described by the following function (Cressie 1993):

$$\gamma'(h,\theta) = \begin{cases} 0 & , \quad h = 0 \\ \theta_n + \theta_s \left(1 - \exp\left(-\frac{h^2}{{\theta_r}^2}\right)\right) & , \quad h \neq 0 \end{cases} \tag{3}$$

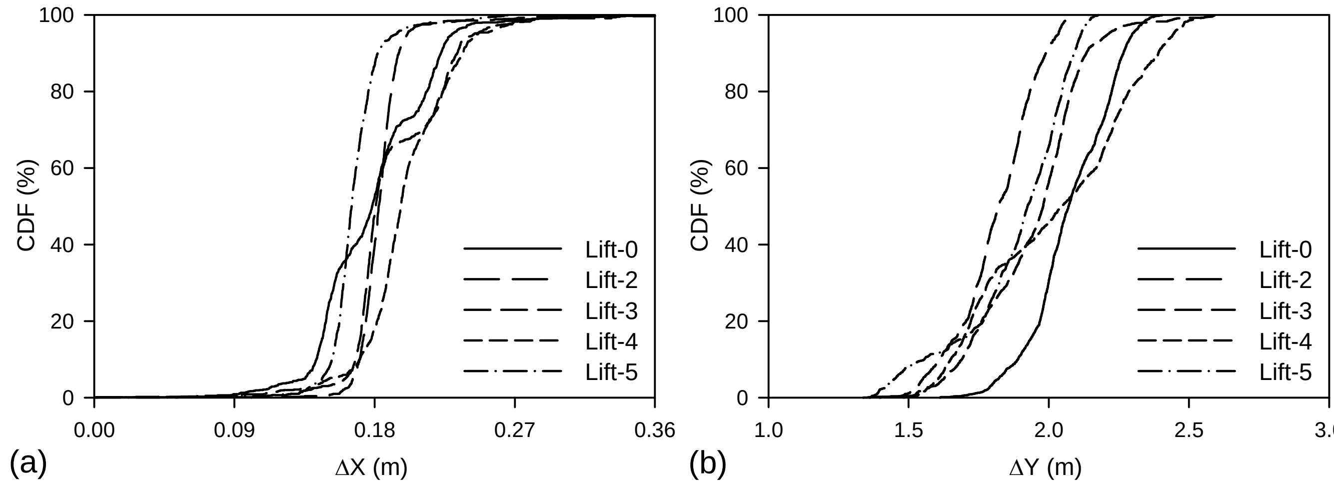

Fig. 2: Cumulative distribution functions of the point-to-point spacings for five lifts of compacted soil, for data collected in the: (a) X direction, and (b) Y direction.

In addition to the spatial distance h, the Gaussian model $\gamma'(h, \theta)$ has three other parameters: the range (θ_r), the nugget (θ_n), and the sill ($\theta_r + \theta_s$), as shown in Fig. 3. In a simplistic semivariogram model, the range is defined as the spatial distance (h), measured from the prediction location, at which point the model reaches the maximum semivariance or sill; at lag spacings greater than the range, the semivariance does not change (i.e., it continues along at a constant value), which generally implies that there is no longer a meaningful correlation between the spatial data. In contrast to simpler semivariogram models, the Gaussian model increases asymptotically toward the sill, never reaching a numerical maximum. In this case, the "effective range" is the distance where the variogram reaches 95% of the sill; for the Gaussian model, the "effective range" is equal to $\sqrt{3}\theta_r$ (e.g., Christakos 1992; Deutsch and Journel 1992). The nugget effect corresponds to the discontinuity that can be present at the origin of the semivariogram. In theory, $\theta_n = 0$, but in reality, because of micro-scale variation, a discontinuity at the origin leads to $\theta_n > 0$ (Cressie 1993). The possible reasons for this discontinuity are measurement errors and errors as a result of rounding spatial distances between pairs of points to the nearest lag distance that is used to define the semivariogram. The sill, which is the sum of θ_n and the partial sill θ_s, is equal to the maximum semivariance of the model.

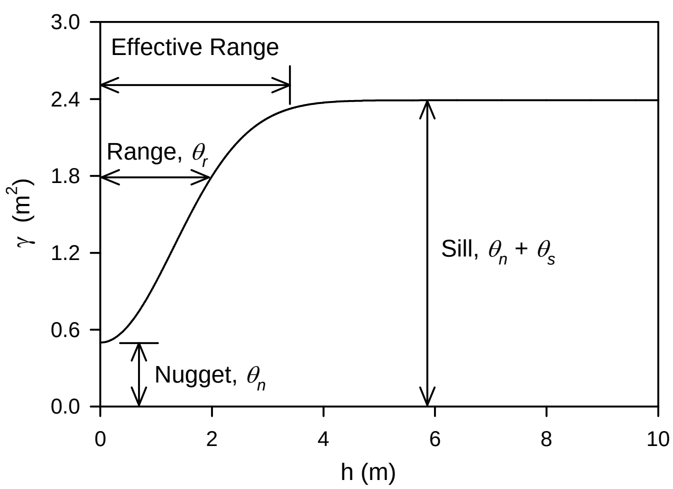

Fig. 3: A typical Gaussian theoretical semivariogram.

6.2 *Investigation of Isotropy/Anisotropy*

To perform kriging, theoretical prediction models derived from empirical semivariograms are needed. As part of the development of an empirical semivariogram, it is necessary to assess whether the data that is being analyzed is isotropic or anisotropic in nature. For isotropic data sets, it is necessary to account for only the magnitude of the distance between points when creating the empirical semivariogram, whereas anisotropic empirical semivariograms require the use of techniques that account for both the magnitude and direction of the distance between data points (e.g., Isaaks and Srivastava 1989). Consequently, omnidirectional semivariograms are used for isotropic data sets, and directional semivariograms are used for anisotropic data sets. A geometric anisotropy model employs semivariograms that approach the same sill, with different ranges in all directions. The weighting functions for geometrical anisotropic kriging are developed using the omnidirectional semivariogram and the ratio between the maximum (major direction) and minimum (minor direction) ranges of all the directional semivariograms. The definition of geometric anisotropy requires that the major and minor directions be perpendicular to each other (e.g., if the maximum range corresponds to the 0° directional semivariogram, then the minimum range will occur in the 90° directional semivariogram) (Budrikaite and Ducinskas 2005). A simple method for evaluating anisotropic behavior is to compare the range of different directional semivariograms. If there is significant difference in the ranges, there may be evidence that the spatial data has a directional dependence (e.g., Budrikaite and Ducinskas 2005; Facas et al. 2010).

For the roller data that was recorded in this study, the directional dependence of the measured data was assessed by looking at the ranges of a large number of directional semivariograms having various orientations. From this analysis, it was observed that the dominant major direction for anisotropic kriging occurred parallel to the roller lane (the X-axis direction), which means that the corresponding minor direction of anisotropy is perpendicular to the roller lane (the Y-axis direction). Figure 4 shows a comparison of the X-directional $\gamma_x(h)$ and the Y-directional $\gamma_y(h)$ empirical semivariograms for the final pass of each compacted soil lift. For the data that was recorded in the current study, the low spatial resolution of measured values in the Y direction made it difficult to determine the range of the Y-directional semivariograms; this is consistent with previous research that has utilized semivariograms for anisotropic analysis of roller measured data (Facas et al. 2010). Consequently, the ratio between the maximum and minimum ranges (corresponding to the major and minor directions of anisotropy) could not be determined. As a result, because of the nature of the data that was recorded in the current study (long roller lanes, with only limited data in the perpendicular direction), it was not possible to perform meaningful anisotropic ordinary kriging. Therefore, the isotropic ordinary kriging method was used to predict lift thickness values. In future studies, the authors recommend that researchers construct a square test pad area that has a much greater sampling point density in the direction perpendicular to the roller's path of compaction; this should allow for more effective assessment of anisotropic kriging analysis tools for application to geospatial interpolation of field lift thickness data.

6.3 *Omnidirectional Semivariogram Model Fitting*

Figure 5 shows the omnidirectional empirical semivariograms for the final pass of each compacted soil lift. As shown in Figs. 4 and 5, some periodicity is observed in the empirical semivariogram data at point spacings past 5-6 m; the cause of this observed behavior is unknown. Also shown in Fig. 5 are the theoretical Gaussian models $\gamma'(h)$ that have been fit to the empirical data points for each lift; the associated model fitting parameters are presented in Table 1. In the current study, these theoretical Gaussian models are used for each lift to determine the weighting functions that are employed during geospatial interpolation of lift elevations using the ordinary kriging method. Grid interpolation results using the isotropic ordinary kriging approach are shown alongside those from the inverse distance weighting method in later sections of this manuscript (e.g., Figs. 6-9).

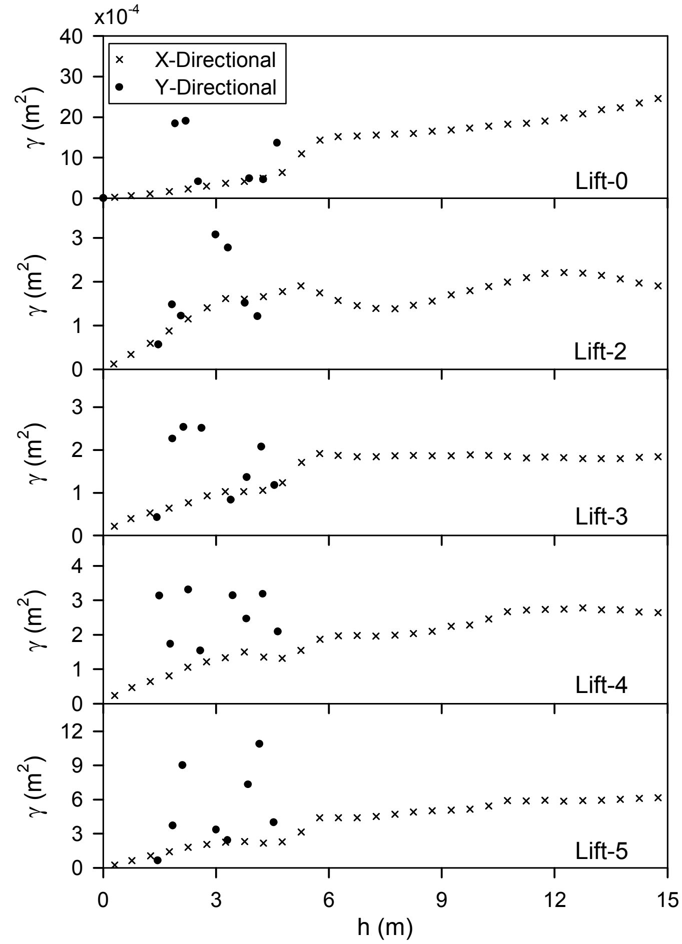

Fig. 4: Comparison of empirical directional semivariograms: X directional versus Y directional.

6.4 *Limitations to Using a Kriging Approach in a Specification Framework*

Kriging methods have been widely used in the area of geospatial prediction, and they are generally considered to be the "state-of-the-art" method for prediction of CCC measured values at unknown points (e.g., White et al. 2007; Tehrani 2009; Mooney et al. 2010; Vennapusa et al. 2010). However, a major drawback to kriging is that it is a somewhat mathematically complex technique that requires that the user have a fairly significant background in statistics, often beyond what is taught in an introductory statistics course at the university level. This presents a problem if this technique is going to be used in the field in real time by field engineers or engineering technicians, as the end users of this tool may lack the necessary mathematical background and/or training to implement it properly. Deployment of kriging tools in "black box" software programs for utilization by untrained field personnel is in particular not recommended by the authors, because of the risk of improper use of kriging.

A second disadvantage of kriging is that it typically requires some judgment on the part of the end-user when fitting theoretical semivariogram models to empirical semi-

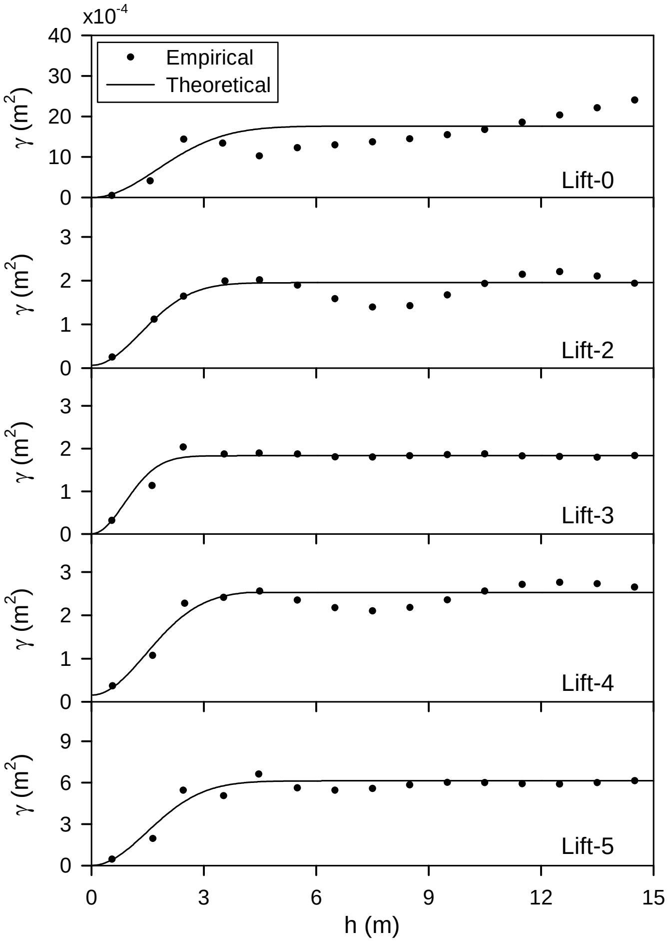

Fig. 5: Empirical omnidirectional semivariograms with fitted theoretical Gaussian models.

variogram data sets. In some cases, this judgment-based fitting is more of an art than a precise science, and different model fits that may be selected by the user can lead to different end results. Further, different users prefer different theoretical semivariogram models, and some users are quicker to move toward anisotropic models than others for data sets that exhibit some anisotropy. Taken together, this variety of judgment-based factors can make user-to-user analysis of a given data set somewhat variable, and potentially opens room for conflicts between the owner and contractor if this technique is to be used as part of a field QA/QC specification framework. Consequently, it is worth exploring the use of simpler interpolation techniques for estimating elevation values at the grid point locations.

7 Interpolation Using the Inverse Distance Weighting Method

An alternative interpolation approach for predicting elevation values at each of the grid point locations is the inverse distance weighting (IDW) method (e.g., Isaaks and Srivastava 1989). In the IDW method, a neighborhood about the interpolated point location is identified and a weighted average is taken of the observation values within this neighborhood. The relative weights (contributions) of neighboring points are assigned based upon their distance from the interpolation point. Although more sophisticated anisotropic analysis techniques or weighted neighborhood approaches (e.g., Shepard's 1968 method) can be employed within an IDW framework, a relatively simplistic isotropic IDW approach was utilized in this paper, with the goal being that it would be as simple to use and understand as possible for field engineers, with little room for debate among contractors and owners. If a more sophisticated approach is needed, the authors recommend kriging using the techniques that are discussed in the previous section. Consequently, to keep the IDW method as simple as possible, a simple inverse power weighting function was utilized, with a neighborhood size that was equal to the domain of the entire data set (Isaaks and Srivastava 1989):

$$w_i(h) = \frac{\sum_{i=1}^{n} \frac{1}{h_i^p} z(x_i)}{\sum_{i=1}^{n} \frac{1}{h_i^p}} \tag{4}$$

where, $h_i ... h_n$ are the distances from each of the n sample locations to the point being estimated, $z(x_1) ... z(x_n)$ are the sample values, and the exponent p is the power weighting function (Isaaks and Srivastava 1989). As shown in Eq. 4, the weighting function that is used is completely dependent upon the exponent value, p. If $p = 1$, a linear decay function is applied to all measured values within the defined neighborhood. Likewise, for $p = 2$, a second-order decay function is used to weight the measured values as a function of h, and so on. Typically, the value of p is chosen by the user through assessment of the spatial data set, using their judgment and experience.

For the roller data that was recorded in this study, the IDW method was applied to the elevation data, with four different exponent values being assessed: $p = 1$, $p = 2$, $p = 4$, and $p = 64$. A cumulative distribution function of the predicted elevation values that result at the grid point locations for different values of p is shown in Fig. 6, for each of the lifts that were assessed. As shown, the selection of p has a fairly significant effect on the analysis results. Also shown in these plots is the CDF of the elevation values that are predicted using an isotropic kriging approach. It can be observed that a value of $p = 4$ tends to yield IDW CDFs that are in the closest agreement with the isotropic kriging results, for the data that was measured in the current study.

Although the CDFs for $p = 4$ tended to agree the most closely with the CDFs for the isotropic kriging results, point-by-point comparisons are also warranted, because the CDFs only show the overall distribution of the data, and not how things compare exactly at each grid point location. Figure 7 shows a direct comparison of IDW-predicted values (using $p = 4$) at each of the lift 2 grid points with those that were predicted using the isotropic kriging approach. The associated RMSE between the values predicted using these two approaches is shown in Fig. 7, and in Table 2 for other values of p, for each of the compacted soil lifts. As shown in Fig. 7 and Table 2, a p value

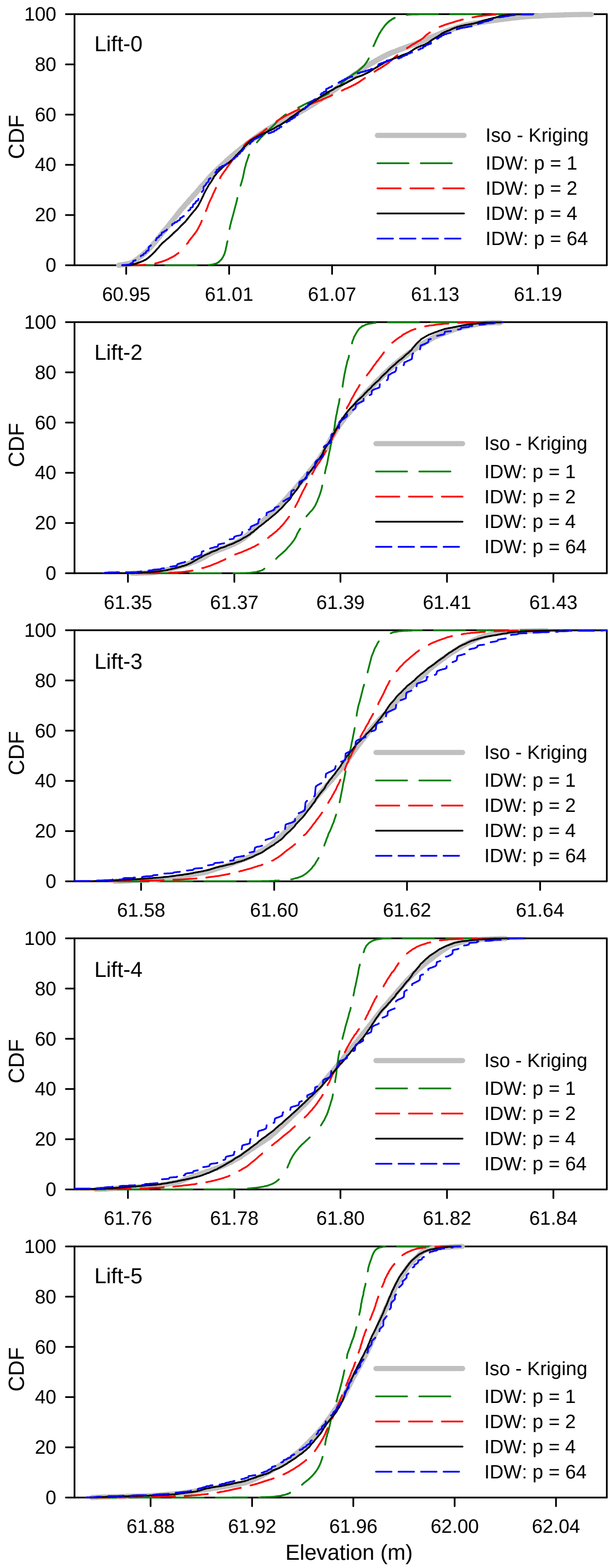

Fig. 6: Cumulative distribution functions of the predicted grid point elevation values for five lifts of compacted soil. Results are presented for interpolation using isotropic kriging and inverse distance weighting with different p values.

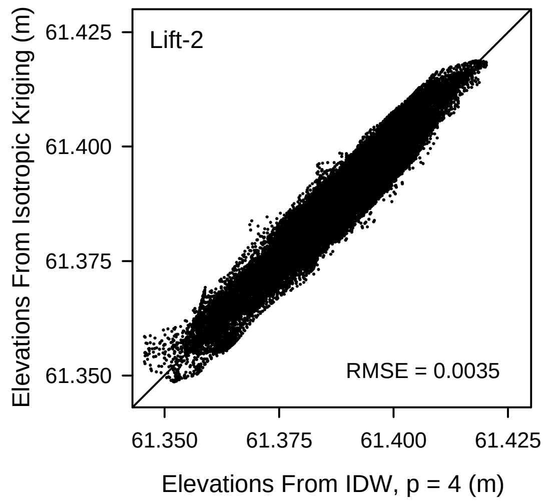

Fig. 7: A comparison of predicted elevation values determined using isotropic kriging and an IDW approach with $p = 4$ (lift 2).

of 4 tended to yield the best agreement between the IDW results and those that were generated using the isotropic kriging interpolation approach, for each of the compacted soil lifts.

A comparison of the CDFs shown in Fig. 6 and the relative RMSE values shown in Table 2 generally seems to support the conclusion that the IDW method with $p = 4$ may be an acceptable substitute for isotropic kriging, for elevation interpolation of "typical resolution" RTK-GPS elevation data. Further studies are needed to support this conclusion, as it is not yet clear if this trend will be consistent across other data sets. For the remainder of this paper, side-by-side results will be presented using isotropic kriging and an IDW approach with $p = 4$, to allow the reader to make their own assessment and comparisons of these two approaches.

8 Determination of Lift Thicknesses

The final compacted thickness of each soil lift can be determined by comparing the interpolated elevation value at each grid point location with the interpolated value at the same grid point location for the underlying lift. Taking the difference in elevation values from lift to lift at each of the grid point locations allows a spatial map of lift thickness to be built. Figure 8 shows the lift thickness maps that result from the data that was collected in this study. For comparison purposes, side-by-side data are shown for an isotopic kriging approach (Fig. 8(a)) and an IDW approach with $p = 4$ (Fig. 8(b)). Figure 9 shows the corresponding CDFs for the spatial data that is presented in Fig. 8. Table 3 provides the mean, standard deviation, and coefficient of variation values for the thickness of each lift.

When examining this data, it should be noted that the "0-2" plots correspond to the thickness of two compacted soil lifts, because of a field malfunction with the data-acquisition system during the placement of the first lift (lift 1, "0-1"). Consequently, the thickness measurements for

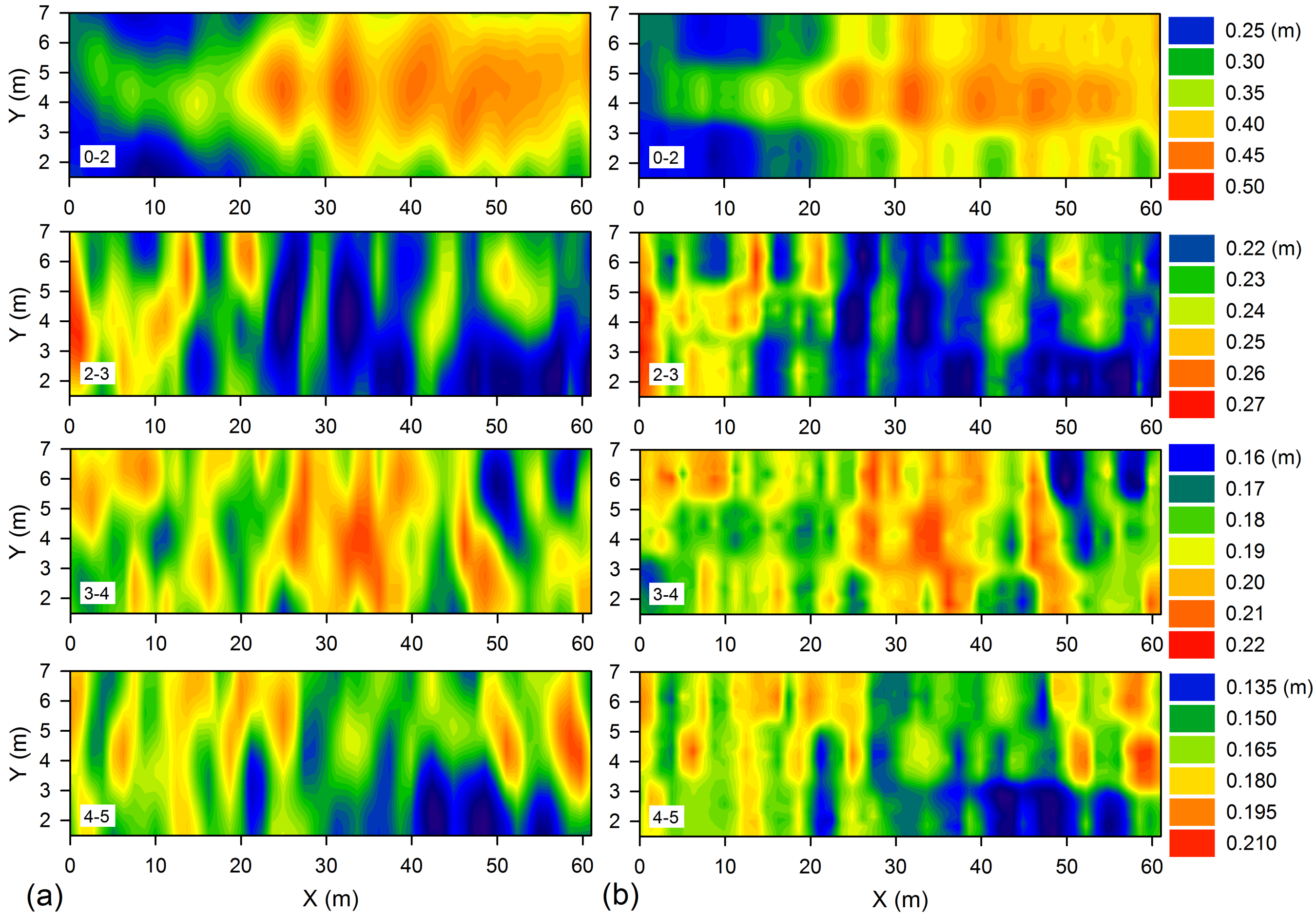

Fig. 8: Contour plots of lift thickness: (a) determined from elevation values interpolated using an isotropic kriging approach, and (b) determined from elevation values interpolated using an IDW approach with $p = 4$.

"0-2" are much larger than those for the other lifts. Also, it should be noted that lifts 1 and 2 ("0-1" and "1-2") were spread manually by a bulldozer operator, whereas lifts 3-5 ("2-3," "3-4," and "4-5") were placed using the same bulldozer with GPS control on the blade of the bulldozer. Furthermore, when placing the base lift in the field, it was also observed that the bulldozer operator tended to fill low areas with thicker soil lifts to achieve a more uniform pad for soil compaction; this is reflected in the data shown in Fig. 8.

As noted previously, the goal of this project was to build a road sub-base embankment to an approximate total final height of 0.9 m (3.0 ft), by compacting five 20.3 cm (8 in.) loose-lift layers. However, actual QA/QC monitoring of loose-lift thickness in the field was much more casual, as is typical of many real field projects; there was simply too much going on to keep track of spreading and loose-lift placement operations at all times, even with a number of experienced field personnel (and most typical sites this size would only have one or two field engineers). However, by examining the mean compacted lift thickness data shown in Table 3, it can generally be observed that the mean after-compaction lift thicknesses were fairly reasonable for the current project. (It should be noted, however, that this observation requires a bit of judgment, as the loose-lift and compacted-lift thickness values are different measures of thickness). The following additional significant observations can also be made from the data shown in Figs. 8 and 9 and Table 3:

1. There is little practical difference in the lift thickness results that are generated from the isotropic kriging and IDW interpolation approaches; this is not surprising, given the fairly close agreement in interpolated elevation values that was noted previously (e.g., Fig. 6, Table 2). Furthermore, and perhaps more importantly, the "thicker areas" and "thinner areas" shown in Fig. 8 are generally the same between the two approaches. This means that either a kriging or IDW approach can be used in the field to build spatial thickness maps to provide the contractor or field QA/QC personnel with feedback about specific areas in compacted soil lifts that may have been placed too thick.
2. This technique provides a good measure of the overall mean thickness of a compacted soil lift, the uniformity of that thickness (via either standard deviation or COV), and the spatial distribution of thick and thin areas (via the spatial mapping technique that is

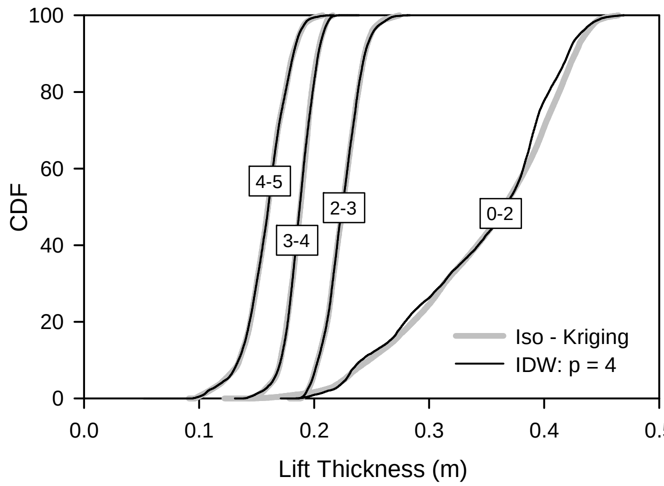

Fig. 9: Cumulative distribution functions showing the variation in thickness of the compacted soil layers. Results are presented for interpolation using isotropic kriging and inverse distance weighting with $p = 4$.

shown in Fig. 8). By examining Figs. 8 and 9, it can be observed that this technique does not yield a lot of single outlier point measurements, but rather fairly smoothed maps of thicker and thinner areas that can be used to guide contractor field operations.

3. Even under carefully controlled research conditions, variable lift thicknesses were observed from lift-to-lift and within a given lift. For real projects that have additional schedule and cost pressures, it would not be surprising if the results were even more variable than what was observed in this study. This observation shows the potential benefit of the approach that is described in this manuscript for performing QA/QC of lift thickness. Future research is needed to quantify how much variability in lift thickness is acceptable as part of "good construction practices" versus "bad construction practices". The techniques presented in this paper provide a framework for quantifying the variability of lift thickness for different types of field projects (e.g., transportation, residential, commercial) and soil placement approaches and technologies (e.g., earthmoving equipment such as bulldozers and graders with and without GPS on the blade). If implemented properly in a specification framework, the approaches outlined herein can yield a better quality finished product, while simultaneously reducing observational demands on field personnel to continuously and directly monitor lift thickness as the soil is being placed.
4. The soil lifts that were spread manually by the bulldozer operator ("0-2") tended to be significantly more variable in thickness than those that were spread with a bulldozer that was equipped with GPS guidance on its blade. This observation lends significant support to the use of GPS feedback and control equipment in conjunction with bladed soil-spreading equipment such as bulldozers and graders.

9 A Discussion of Thickness Measurements, Their Accuracy, and the Effect of this Accuracy on Specification Implementation

The QA/QC technique that is proposed herein uses RTK-GPS-measured roller position values in conjunction with grid interpolation with either a kriging or an IDW approach to build spatial maps of lift thickness. This technique can potentially be used to monitor either "loose lift" or "compacted lift" thicknesses. The use of this technique with compacted lift thicknesses is demonstrated in this paper. If this technique is going to be used within a loose-lift specification framework, users should be aware that, as the first roller pass for a given lift does compact the soil, measurements made using first-pass RTK-GPS roller data do not provide a truly representative measure of the loose-lift thickness. If a "loose-lift" thickness measurement is truly desired, it would probably be more appropriate to use RTK-GPS values that are measured off of bladed soil-spreading equipment such as bulldozers and graders, at the end of spreading and prior to any compaction of the soil. However, based upon our experience with the current study, the authors feel that a compacted lift specification requirement will provide a better measure and indicator of future compacted lift performance; this type of RTK-GPS monitoring data can best be obtained from QA/QC roller measurements that are made during the final pass of compaction for each lift (as was done in the current study).

For the methodology proposed herein to be effective, it needs to be incorporated into a QA/QC specification framework to control the process of soil compaction. Prior to this point, additional research is needed to identify target levels of acceptability for "good construction practices" and "bad construction practices." Further research is also needed to develop a better understanding of the effect that RTK-GPS measurement accuracy has on lift thickness measurements, and to determine whether there are any particular receiver mounting positions (i.e., cab, drum center, or two receivers on either end of the drum) that yield superior measurement results. Once target levels of acceptability for "good construction practices" and "bad construction practices" have been defined and the effect of measurement error and receiver mounting position on the device results is better understood, incentives and penalties can be built into the specification framework to ensure good construction practices.

In essence, the methodology proposed herein suggests the use of RTK-GPS equipment for performing a field survey of soil lift elevation. No discussion of surveying would be complete without a discussion of accuracy, and it is worthwhile here to discuss the possible effects of measurement uncertainty, because of the effect that this factor can have on implementation of this technique within a specification framework.

Conventional RTK-GPS manufacturer specifications cite nominal accuracy for their dual-frequency GPS systems that are on the order of ±1 cm+2 ppm for horizontal position measurements and ±2 cm+2 ppm for vertical position measurements; independent verification of these accuracy levels has shown that they are generally correct within reasonable survey distances from the base station unit (e.g., Lemmon and Gerdan 1999). Many vendors also indicate that the more satellites that are being received, the better the measurement accuracy will be, which seems logical given the general operating principles of GPS technology. Interestingly, Lemmon and Gerdan (1999) reported that, for field surveys conducted where the GPS satellite counts ranged between 5 and 9, an increase in satellites made no significant contribution to the accuracy of the RTK positions (although the reliability of the ambiguity resolution process did improve).

With RTK-GPS systems, a secondary receiving station is set up in the near vicinity of the survey area. This receiving station, which is typically called a "base station", is set up over a known, surveyed point, and its primary function is to eliminate survey errors caused by the earth's atmosphere. As the base station receives GPS satellite information, it compares that data to its known location and continually transmits correction data to the "roving" GPS receivers and GPS machine control units that are located at the job site. This local correction data allows the roving units to calculate their "relative" position often to an accuracy level of a few millimeters.

In general, the "relative" position accuracy of various roving units that are measured with an RTK-GPS unit that has a base station setup has not been as well quantified by manufacturers or researchers, as the accuracy of relative position measurements is more difficult to directly ascertain. However, most manufacturers and researchers generally agree that local coordinate measurements made by RTK-GPS systems (e.g., relative position measurements) are generally more accurate than the absolute accuracy values that are quoted by GPS manufacturers. In general, the absolute accuracy of RTK-GPS measurements is also limited by the accuracy of the field survey that was used to determine the position of the base station.

In any case, it is not overly productive to get caught up in a detailed discussion of whether the accuracy level of RTK-GPS systems is a few millimeters or a few centimeters. RTK-GPS systems are generally accepted to be accurate enough for "rough" survey control. Moreover, the approach that is proposed herein is significantly more accurate than the current state of practice for field QA/QC of lift thickness.

If the agency or agent responsible for QA/QC has concerns about how the potential measurement accuracy of RTK-GPS systems could be drawn into a contentious debate between an owner and contractor, or how this discussion of uncertainty error might play out in a penalty or incentive framework (or worse yet, in a courtroom setting), the solution is a fairly simple one: If you want an 18-cm-thick lift at the end of compaction, only penalize the contractor for areas of the lift that are thicker than 20 or 21 cm. Also, in the specification, be sure to specify a minimum number of satellites that must be maintained (five seems reasonable, corresponding to the observations made by Lemmon and Gerdan 1999), and require that the data-acquisition system actively record the number of satellites for each position point measurement that is made. This takes the question of accuracy off the table, while keeping the big picture in mind - after all, what is the real goal here? To catch lifts that are being placed at 150% or 200% of their maximum specified lift thickness, not 105%, e.g., the "bad offenders" in the soil compaction process that will likely lead to performance-related problems in the long term.

If nothing else, perhaps the most important point to make here is that, if deployed properly, the methodology that is proposed in this paper will "do no harm." That is, we now have a tool that could be used to identify potential problem areas, particularly areas that are in gross violation of lift thickness placement requirements. If there is a real concern about the accuracy of the RTK-GPS equipment, once these problem areas are identified, other more traditional tools (manual measurements, high-accuracy field surveying, etc.) can be deployed to assess the significance of the problem.

10 Summary and Conclusions

A critical and often overlooked area when performing quality assurance and/or quality control of soil compaction is the specification for maximum lift thickness. This criterion plays an important role in both "method-based" and "end-product-based" soil compaction specifications. In most cases, current practice relies on a visual "eyeball-check" of the maximum lift thickness by the field inspector; in some cases, the field inspector will measure the height of the lift at a limited number of locations to the best of his or her ability. Field surveys from lift to lift are relatively uncommon. Consequently, a large percentage of the fill area is typically placed at thicknesses that are not verified in a reliable and regularly quantifiable way.

Recent research has indicated that compaction control is likely moving toward the use of "smart" intelligent compaction (IC) or continuous compaction control (CCC) rollers that continuously record indicator measurements that provide information about the stiffness of compacted soils. As part of this process, these rollers are outfitted with real-time kinematic global-positioning system (RTK-GPS) equipment that measures the position (X, Y, Z) of the compacter in real time. This paper provides a framework for using field RTK-GPS measurements made by CCC or IC equipment to monitor and control the thickness of compacted soil lifts during construction of a roadway embankment. The procedure that is proposed involves the following steps:

1. Continuously record compactor position information (X, Y, Z data) for two (or more) consecutively compacted soil lifts. As part of normal field CCC procedures, position data should be recorded for each compactor pass in a given lift; however, it is only necessary to compare data collected from the final pass of compaction for two consecutive soil lifts.
2. Create a "projection grid" to compare elevation mea-

surements for two consecutive lifts. This projection grid should be isotropic, with a grid point spacing that is near the lower bound of the measured point spacing distances in the roller measured direction (the X direction). Based on the data recorded in this study, this value will typically be approximately half of the mean spacing between points in the roller-measured direction.

3. Use an interpolation technique to infer elevation values at each of the grid point locations for the entire projection grid, from the measured elevation (Z) data for the final pass of compaction for each lift. Based on the results from the current study, either an isotropic kriging approach or an inverse distance weighting (IDW) approach with $p = 4$ can be used for this purpose. The IDW method is recommended, as it is simpler to apply in a field setting, and the results were not observed to differ substantially from the more sophisticated kriging approach.
4. Determine the spatially varying thickness of each compacted soil lift by taking the difference in elevation values from lift to lift at each of the projection grid point locations. Plot either a histogram or cumulative distribution function of the thickness data for the lift, determine the mean lift thickness, and a statistical measure of its variability such as the standard deviation or coefficient of variation. If the mean lift thickness or lift thickness variability appears too high, plot a spatial map (traditional contour plots or color-coded contour plotting techniques can be useful for visualization purposes in this step). If necessary, from the spatial map, identify problem areas for the contractor to address prior to moving on to the next lift.

This proposed QA/QC technique can be effectively used to monitor compacted soil lift thicknesses, as demonstrated in this paper with data collected from a full-scale field study. The proposed technique successfully addresses one of the obstacles associated with using GPS measurements for field monitoring of lift thickness, the problem of varying roller position from lift to lift. Future research using CCC rollers is needed to quantify target levels of acceptability for "good construction practices" and "bad construction practices," prior to development of specifications that utilize this approach. Further research is also needed to develop a better understanding of the effect that RTK-GPS measurement accuracy has on lift thickness measurements. Once target levels of acceptability for "good construction practices" and "bad construction practices" have been defined and the effect of measurement error on the device results is better understood, incentives and penalties can be built into the specification framework to ensure good construction practices.

As an added advantage, the roller surveys that are conducted and accompanying spatial data maps that can be constructed using the analytical approach outlined herein have interesting potential for creating "as-built" survey maps of compacted soil areas that can be used with enhanced real-time construction data networks, such as within the framework of "BIM" (building information management) for geotechnical construction.

As a final word of caution, the findings from the current study should not be extrapolated out to other CCC applications without performing similar sensitivity analyses to those that are presented and discussed in the current paper. In particular, geospatial analysis of stiffness indicator values that are commonly measured by CCC/IC equipment (such as CMV or MDP, e.g., Meehan and Tehrani 2011) require separate assessment of their geospatial behavior than what is presented herein for lift thickness. For example, some vibratory-measured stiffness indicator values have been shown to exhibit anisotropic tendencies (e.g., Facas et al. 2010).

Acknowledgments

This material is based on work supported by the Delaware Department of Transportation under Award Nos. 11A00133, 09000112, and 07000704. The writers would like to express their gratitude to the Delaware Department of Transportation; Caterpillar, Inc.; and Greggo & Ferrara, Inc. for supporting this study with valuable manpower and equipment donations. In addition, the writers would like to thank James Pappas, Nicholas Ferrara III, Jim Reynolds, Al Strauss, Dean Potts, Richard Costello, AJ Lee, Nick Oetken, Mario Souraty, and Dan Sajedi for their valuable assistance with the field study and associated data analysis. The writers would also like to thank the geotechnical graduate students at the University of Delaware who patiently helped us to accomplish the fieldwork for this study in a timely fashion: Farshid Vahedifard, Majid Khabbazian, Yueru Chen, Baris Imamoglu, and Fan Zhu. The writers also thank Faraz Tehrani for his valuable assistance with interpretation of the data that is presented herein. Finally, Christopher L. Meehan would like to acknowledge the support of the Fulbright Center in Finland and the 2012-2013 Fulbright-Tampere University of Technology Scholar Award, which provided support for work on this manuscript.

References

Adam, D., 1997, "Continuous Compaction Control with Vibratory Rollers," *GeoEnvironment 97*, Rotterdam, The Netherlands, pp. 245-250.

Adam, D. and Brandl, H., 2003, "Sophisticated Roller Integrated Continuous Compaction Control," *12th Asian Regional Conference on Soil Mechanics and Geotechnical Engineering*, Vol. 1, Aug. 4-8, Singapore, World Scientific, Singapore, pp. 427-430.

Adam, D., 2007, "Roller Integrated Continuous Compaction Control CCC Technical Contractual Provisions and Recommendations," *Design and Construction of Pavements and Rail Tracks: Geotechnical Aspects and Processed Materials*, A. G. Correia, Y. Momoya, and F. Tatsuoka, Eds., CRC, Boca Raton, FL, pp. 111-138.

Anderegg, R., von Felten, D., and Kaufmann, K., 2006, "Compaction Monitoring Using Intelligent Soil Compactors," *Proceedings of the Geo-Congress 2006: Geotechnical Engineering in the Information Technology Age*, Atlanta, GA, February 26 - March 1, 2006, ASCE, Reston, VA.

Brandl, H. and Adam, D., 1997, "Sophisticated Continuous Compaction Control of Soils and Granular Materials," *Proceedings of the 14th International Conference on Soil Mechanics and Foundation Engineering*, Balkema, Rotterdam, The Netherlands, September 6-12, pp. 1-6.

Budrikaite, L. and Ducinskas, K., 2005, "Modeling of Geometric Anisotropic Spatial Variation," *Proceedings of the 10th International Conference MMA 2005 and CMAM2*, Trakai, Technika, Lithuania, June 1-5, pp. 361-366.

Christakos, G., 1992, *Random Field Models in Earth Sciences*, Academic Press, San Diego, CA.

Clark, I. and Harper, W., 2002, *Practical Geostatistics 2000*, Ecosse North America, Columbus, OH.

Cressie, N. A. C., 1993, *Statistical Methods for Spatial Data Analysis*, revised ed., Wiley, New York.

DelDOT, 2001, "Specifications for Road and Bridge Construction," Prepared by The Delaware Department of Transportation, Nathan Hayward III, and Raymond M. Harbeson, August.

Deutsch, C. V. and Journel, A. G., 1992, *GSLIB: Geostatistical Software Library and Users Guide*, Oxford University Press, Oxford, NY.

Facas, N., Mooney, M., and Furrer, R., 2010, "Anisotropy in the Spatial Distribution of Roller-Measured Soil Stiffness," *Int. J. Geomech.*, Vol. 10, pp. 129-135.

Floss, R., Gruber, N., and Obermayer, J., 1983, "A Dynamical Test Method for Continuous Compaction Control," *Proceedings of the 8th European Conference on Soil Mechanics and Foundation Engineering*, H. G. Rathmayer and K. Saari, Eds., Balkema, The Netherlands, pp. 25-30.

Forssblad, L., 1980, "Compaction Meter on Vibrating Rollers for Improved Compaction Control," *Proceedings of the International Conference on Compaction*, Vol. 2, Paris, France, pp. 541-546.

Isaaks, E. H. and Srivastava, R. M., 1989, *An Introduction to Applied Geostatistics*, Oxford University Press, New York.

Lemmon, T. R. and Gerdan, G. P., 1999, "The Influence of the Number of Satellites on the Accuracy of RTK GPS Positions," *Austr. Surveyor*, Vol. 44(1), pp. 64-70.

Meehan, C. L. and Tehrani, F. S., 2011, "A Comparison of Simultaneously Recorded Machine Drive Power and Compactometer Measurements," *Geotech. Testing J.*, Vol. 34(3), pp. 208-218.

Meehan, C. L., Tehrani, F. S., and Vahedifard, F., 2012, "A Comparison of Density-Based and Modulus-Based In Situ Test Measurements for Compaction Control," *Geotech. Testing J.*, Vol. 35(3), pp. 387-399.

Mooney, M., Rinehart, R., Facas, N., Musimbi, O., White, D., and Vennapusa, P., 2010, "Intelligent Soil Compaction Systems," *NCHRP Report 676*, Transportation Research Board, Washington, D.C.

Olea, R. A., 2006, "A Six-Step Practical Approach to Semivariogram Modeling -Teaching Aid," *Stoch. Environ. Res. Risk Assess.*, Vol. 20, pp. 307-318.

R Development Core Team, 2011, "R: A Language and Environment for Statistical Computing," R Foundation for Statistical Computing, Vienna, Austria.

Samaras, A. A., Lamm, R., and Treiterer, J., 1991, "Application of Continuous Dynamic Compaction Control for Earthworks in Railroad Construction," *Transport. Res. Rec.*, Vol. 1309, pp. 42-46.

Shepard, D., 1968, "A Two-Dimensional Interpolation Function for Irregularly-Spaced Data," *Proceedings of the 23rd National Conference ACM*, Aug. 27-29, Las Vegas, NV, ACM, pp. 517-524.

Tehrani, F. S., 2009, "An Investigation of Continuous Compaction Control Systems," M.C.E. thesis, University of Delaware, Newark, DE.

Thompson, M. and White, D. J., 2008, "Estimating Compaction of Cohesive Soils from Machine Drive Power," *J. Geotech. Geoenviron. Eng.*, Vol. 134(12), pp. 1771-1777.

Thurner, H. and Sandström, A., 1980, "A New Device for Instant Compaction Control," *Proceedings of the International Conference on Compaction*, Vol. 2, Paris, France, pp. 611-614.

Vennapusa, P., White, D. J., and Morris, M., 2010, "Geostatistical Analysis for Spatially Referenced Roller-Integrated Compaction Measurements," *J. Geotech. Geoenviron. Eng.*, Vol. 136(6), pp. 813-822.

White, D. J., Jaselskis, E. J., Schaefer, V. R., and Cackler, E. T., 2005, "Real-Time Compaction Monitoring in Cohesive Soils from Machine Response," *Transport. Res. Rec.*, Vol. 1936, pp. 173-180.

White, D. J. and Thompson, M., 2008, "Relationships Between In-Situ and Roller-Integrated Compaction Measurements for Granular Soils," *J. Geotech. Geoenviron. Eng.*, Vol. 134(12), pp. 1763-1770.

White, D. J., Thompson, M., and Vennapusa, P., 2007, "Field Validation of Intelligent Compaction Monitoring Technology for Unbound Materials," *Final Report MN/RC-2007-10*, Department of Transportation, St. Paul, MN.

White, D. J., Vennapusa, P., and Gieselman, H., 2011, "Field Assessment and Specification Review for Roller-Integrated Compaction Monitoring Technologies," *Advances in Civil Engineering*, Hindawi, New York, pp. 1-15.

Table 1: Theoretical Semivariogram Model Fit Parameters

Lift	Range (m)	Partial Sill (m^2)	Nugget (m^2)	Sill (m^2)
0	2.48	0.00176	4.13×10^{-7}	0.00176
2	1.86	0.00019	6.80×10^{-6}	0.00020
3	1.25	0.00018	6.75×10^{-7}	0.00018
4	2.05	0.00024	1.58×10^{-5}	0.00026
5	2.09	0.00061	1.91×10^{-6}	0.00061

Table 2: Root-Mean-Square Error Between Predicted Elevation Values Determined Using an Isotropic Kriging Approach and an Inverse Distance Weighting Approach

	RMSE Between Isotropic Kriging and the Elevation Interpolation Approaches Shown			
Lift	IDW ($p = 1$)	IDW ($p = 2$)	IDW ($p = 4$)	IDW ($p = 64$)
0	0.0329	0.0185	0.0146	0.0175
2	0.0102	0.0054	0.0035	0.0050
3	0.0092	0.0049	0.0039	0.0063
4	0.0108	0.0059	0.0050	0.0074
5	0.0170	0.0089	0.0067	0.0098

Table 3: Mean, Standard Deviation, and Coefficient of Variation Values for the Thickness of Each Lift

	Isotropic Kriging			IDW, With $p = 4$		
Layer	Mean (m)	Standard Deviation (m)	COV (%)	Mean (m)	Standard Deviation (m)	COV (%)
0-2	0.3500	0.0675	19.29	0.3467	0.0655	18.88
2-3	0.2246	0.0156	6.97	0.2246	0.0158	7.05
3-4	0.1870	0.0129	6.87	0.1871	0.0132	7.05
4-5	0.1584	0.0192	12.10	0.1584	0.0193	12.15